

Investigating the Formation Mechanisms of $\text{Cu}_{0.83}\text{Si}_{0.17}$ Intermetallic Phase Formed at Cu-Si and Cu-(5at%)Nb/Si Interfaces

Hüsniye GÜLER^{1*}, Macit ÖZENBAŞ²

¹ *Gazi University KOSGEB Technology Development Center, Beşevler, 06500, Ankara, TURKEY*

² *Middle East Technical University, Department of Metallurgical and Materials Engineering,
06531, Ankara, TURKEY*

Received: 27.12.2010 Revised: 28.03.2011 Accepted: 19.04.2011

ABSTRACT

A study of intermetallic compound formation at the interface between copper thin film and silicon substrate is presented in this work. Two systems; Cu/Si and Cu-(5at%) Nb/Si, were studied. From the intermetallics formed at the interfaces of two systems; as a model, formation mechanisms of $\text{Cu}_{0.83}\text{Si}_{0.17}$ with and without niobium impurity were examined. Variations in values of parabolic rate constants and activation energies with Nb impurity content were determined. The samples were annealed at different temperatures and time intervals after vacuum deposition of the films. X-Ray, Scanning Electron Microscopy (SEM), and Energy Dispersive Spectroscopy (EDS) analysis showed the sequential formation of several intermetallic phases at the interfaces. Using this data, a model had been given about the formation of the observed intermetallic phases.

Key Words: *Intermetallics, thin metal films, impurity effect, reaction rate constants.*

1. INTRODUCTION

Thin films had found usage area in different subjects from electronics, textile to glass and dye industry and related works are being carried on. [1-4] Titanium dioxides's self-cleaning effect has been broadly used in textiles, paints, windows, residual water treatment, amongst various other photocatalytic applications. Polymer substrates have found their way in the semiconductor industry as a base layer for flexible electronics, as well as in sensor and actuator applications[5]. In lithium-ion batteries, nanocrystalline

intermetallic alloys, nanosized composite materials, carbon nanotubes, and nanosized transition-metal oxides are all promising new anode materials, while nanosized LiCoO_2 , LiFePO_4 , LiMn_2O_4 , and LiMn_2O_4 show higher capacity and better cycle life as cathode materials than their usual larger-particle equivalents [6]. The films; layer by layer deposition of zirconium oxide onto silicon, have been studied for their dielectric properties to understand the parameters leading to dense films with high dielectric constant [7]. Due to the increasing use of thin films in

*Corresponding author, e-mail: husniyeguler@gmail.com

electronics, either as complete thin film circuits or more generally as interconnections & contacts in integrated circuits; diffusion in thin films has received significant attention [8-15]. Agillan and his friends determined that when thicknesses of CuInSe₂ thin films increases activation energies of the films decreases [16]. Quang PH and Yu SC investigated effect of substrate temperature to the activation energy of Al_{0.87}Mn_{0.13}N thin film and concluded that activation energy of the film decreases with increased substrate temperature [17]. M.A. Aksu, M.E. Yakıncı and A. Güldeste showed that Co addition to MgB₂ thin film decreases in activation energy. [18] Fadel M, Sedeek K and Hegab NA concluded that Sn addition to Ge_{1-x}Sn_xSe₃ thin film decreases activation energy [19]. Copper thin films are being investigated for the importance in microelectronic devices. Intermetallic compound formation at the interface between copper thin film and silicon substrate is presented in this work. Two systems; Cu/Si and Cu-(5at%)Nb/Si, were studied.

2. EXPERIMENTAL OVERVIEW

Substrates preparation, vacuum coating of these substrates with evaporant, heat treatment of the films, examining the phases formed at the Cu/Si or Cu-(5at%)Nb/Si interface by using X-Ray Diffraction and investigating the surface morphology and microstructure of the film samples, SEM and EDS techniques were followed. The vacuum chamber loaded with evaporant (Cu or Cu-(5at%)Nb were used as evaporant) after silicon substrates cleaned with acetone. These films obtained by evaporating Cu or Cu-(5at%)Nb under vacuum around 10⁻⁵ torr with small fluctuations in a vacuum deposition

unit (Nanotech Thin Films Ltd., Model Microprep 300-S, Manchester, UK) [20].

Cu-(5at%)Nb alloy casting was achieved under argon gas atmosphere at about 1800 °C by using a centrifugal casting machine, Manfredi Neutromag Digital. Cu and Nb were melted by induction heating by using ceramic based sintered special crucible having 2.564 cm³ maximum capacity in the steel mold. During casting water cooled copper coils were used and temperature was measured by pyrometer. After coating; the films were annealed in a horizontal alumina tube furnace equipped with a programmable controller (ABB Kent Taylor-Commander 3000) under argon gas flow with annealing times ranging from 2 hours to 4 hours at temperatures between 400-600°C. The heating and cooling rates were set to +10°C/min and -1.5°C/min, respectively.

3. RESULTS AND DISCUSSION

3.1. Cu/Si System

Cu films having 0.68µm thickness were deposited on silicon substrates and they were annealed at different temperatures; 400°C, 500°C and 600°C for 2 h, 2.5 h, 3 h, 3.5 h and 4 h. Intermetallic phases; Cu_{0.83}Si_{0.17}, Cu₄Si, (Cu, Si)η formed sequentially at the film-substrate interface. The forth layer; (Cu, Si)(Si at%21.2), formed when Cu film was annealed at 600°C for 2.5 h, addition to those three layers which were annealed at 500°C for 3.5 h. These layers were identified from X-Ray, SEM micrograph and EDS spectra. Phases formed at the interface are shown in Table 1.

Table 1. Phases formed during annealing of Cu films on Si substrates for different temperatures and times (constant thickness of 0.680 µm).

No	Heat Treatment	Phases Observed
1	As-deposited	Cu and Silica
2	400°C, t=2 h	Cu _{0.83} Si _{0.17} , Cu ₄ Si, (Cu, Si)η
3	400°C, t=2.5 h	Cu, Cu _{0.83} Si _{0.17} , Cu ₄ Si, (Cu, Si)η
4	400°C, t=3 h	Cu _{0.83} Si _{0.17} , Cu ₄ Si, (Cu, Si)η
5	400°C, t=3.5 h	Cu, Cu _{0.83} Si _{0.17} , Cu ₄ Si, (Cu, Si)η, SiO ₂
6	400°C, t=4 h	Cu, Cu _{0.83} Si _{0.17} , Cu ₄ Si, (Cu, Si)η
7	500°C, t=2 h	Cu _{0.83} Si _{0.17} , Cu ₄ Si, (Cu, Si)η, SiO ₂
8	500°C, t=2.5 h	Cu _{0.83} Si _{0.17} , Cu ₄ Si, (Cu, Si)η, SiO ₂
9	500°C, t=3 h	Cu _{0.83} Si _{0.17} , Cu ₄ Si, (Cu, Si)η, SiO ₂
10	500°C, t=3.5 h	Cu, Cu _{0.83} Si _{0.17} , Cu ₄ Si, (Cu, Si)η, (Cu, Si)(Si at%21.2)
11	500°C, t=4 h	Cu _{0.83} Si _{0.17} , Cu ₄ Si, (Cu, Si)η, (Cu, Si)(Si at%21.2), SiO ₂
12	600°C, t=2 h	Cu _{0.83} Si _{0.17} , Cu ₄ Si, (Cu, Si)η, SiO ₂
13	600°C, t=2.5 h	Cu _{0.83} Si _{0.17} , Cu ₄ Si, (Cu, Si)η, (Cu, Si)(Si at%21.2), SiO ₂
14	600°C, t=3 h	Cu _{0.83} Si _{0.17} , Cu ₄ Si, SiO ₂
15	600°C, t=3.5 h	Cu _{0.83} Si _{0.17} , Cu ₄ Si, SiO ₂
16	600°C, t=4 h	Cu _{0.83} Si _{0.17}

X-Ray diffractograms of Cu films grown on silicon substrate, as-deposited and annealed for 2 h, 2.5 h, 3 h, 3.5 h and 4 h at 500°C, shown in Figure 1. From the intermetallics formed at the interface as an example, growth kinetics of Cu_{0.83}Si_{0.17}; which occurred first as shown in Figure 2.a by number 1, was examined. EDS spectrum of the first layer and second layer are also

shown in Figure 2.b and 2.c. SEM micrograph of 0.68 μm thick Cu film grown on silicon substrate annealed for 3.5 h at 500°C showing the 1st, 2nd and 3rd layers is given in Figure 3.a. EDS spectra of the same film showing the general elemental distribution belongs to these three layers are shown in Figure 3.b, 3.c and 3.d. The thickness measurements of Cu_{0.83}Si_{0.17} phase were carried out by using SEM micrographs.

Cu/Si System

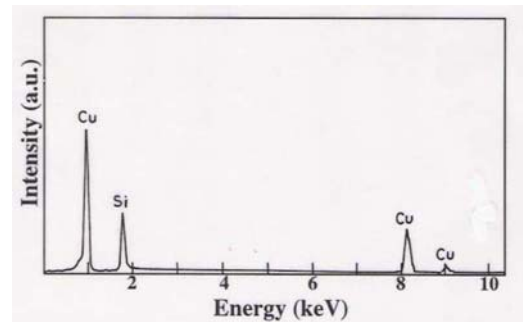
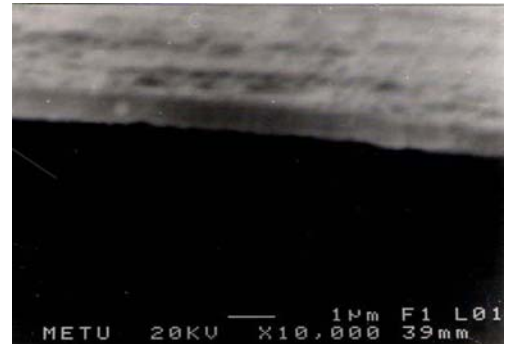
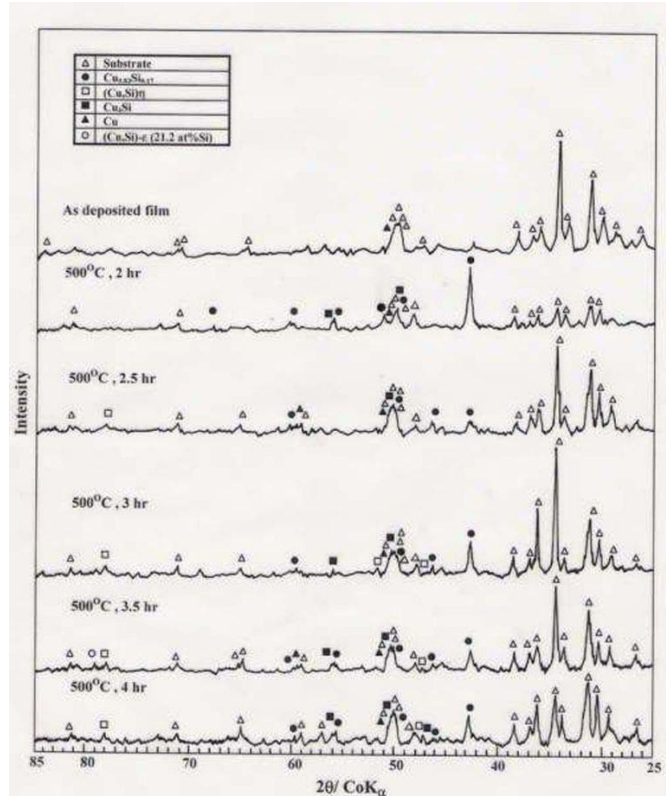


Figure 1 .a-) X-Ray diffractograms of Cu films grown on silicon substrate, as-deposited and annealed for 2 h, 2.5 h, 3 h, 3.5 h and 4 h at 500°C; b-) SEM micrograph of 0.68 μm thick Cu film grown on silicon substrate as-deposited; c-) EDS spectrum of the same film.

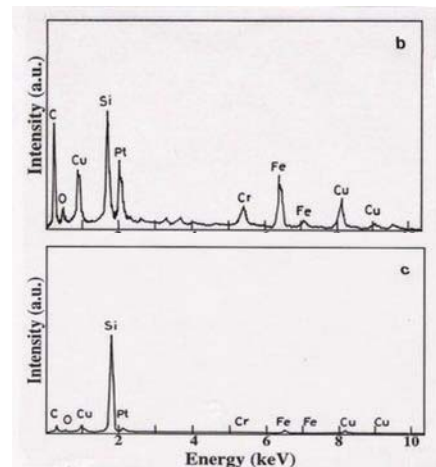
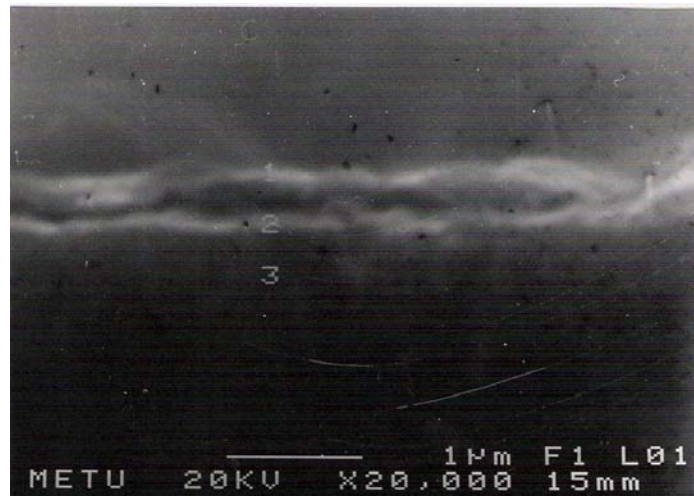


Figure 2.a-) SEM micrograph of 0.68 μm thick Cu film grown on silicon substrate annealed for 2.5 h at 500°C showing the 1st, 2nd and 3rd layers. EDS spectrum of the same film showing the general elemental distribution which belongs to b-) 1st layer, c-) 2nd layer.

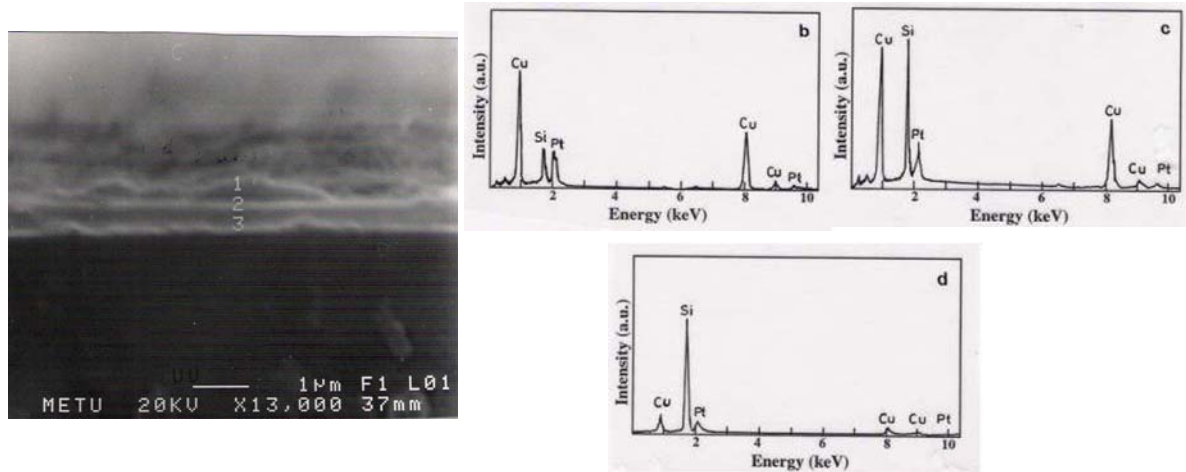


Figure 3. a-) SEM micrograph of 0.68 μm thick Cu film grown on silicon substrate annealed for 3.5 h at 500^oC showing the 1st, 2nd and 3rd layers. EDS spectrum of the same film showing the general elemental distribution which belongs to b-) 1st layer, c-) 2nd layer, d-) 3rd layer.

Table 2 shows thickness variation of $\text{Cu}_{0.83}\text{Si}_{0.17}$ layer with time and temperature. It can be seen that thicknesses of the $\text{Cu}_{0.83}\text{Si}_{0.17}$ layers increase with increasing time and temperatures. Meanwhile; thickness measurements; for

the samples annealed at 400^oC for 2 and 2.5 h, weren't be able to taken because of poor resolution and we got only three data.

Table 2. Thickness variation in μm with time and temperature of $\text{Cu}_{0.83}\text{Si}_{0.17}$ layer in Cu / Si system.

Temp.	time				
	2 h	2.5 h	3 h	3.5 h	4 h
400 ^o C	0.13	0.15	0.16
500 ^o C	0.08	0.11	0.16	0.19	0.23
600 ^o C	0.17	0.24	0.31	0.38

The square of measured phase layer thickness of $\text{Cu}_{0.83}\text{Si}_{0.17}$ versus diffusion time is plotted on a double logarithmic scale for the temperatures; 400^oC, 500^oC and 600^oC as shown in Figure 4. The deviation in the graphic for the sample annealed at 400^oC can be explained by insufficient data. Nonetheless, experimental points were found to lie on a straight line which implies that reactive

diffusion obeys parabolic kinetics and can be expressed by $h^2=k.t$; where h is the thickness of $\text{Cu}_{0.83}\text{Si}_{0.17}$ phase, k is the parabolic rate constant, and t is the diffusion annealing time. Parabolic rate constants were determined by the standard method of least squares analysis together with probable errors as in the following;

$$k_1=1.706 \pm 0.06 \times 10^{-14} \text{ cm}^2/\text{s} \text{ for } 400^{\circ}\text{C}$$

$$k_2=1.972 \pm 0.36 \times 10^{-14} \text{ cm}^2/\text{s} \text{ for } 500^{\circ}\text{C}$$

$$k_3=7.155 \pm 1.24 \times 10^{-14} \text{ cm}^2/\text{s} \text{ for } 600^{\circ}\text{C}.$$

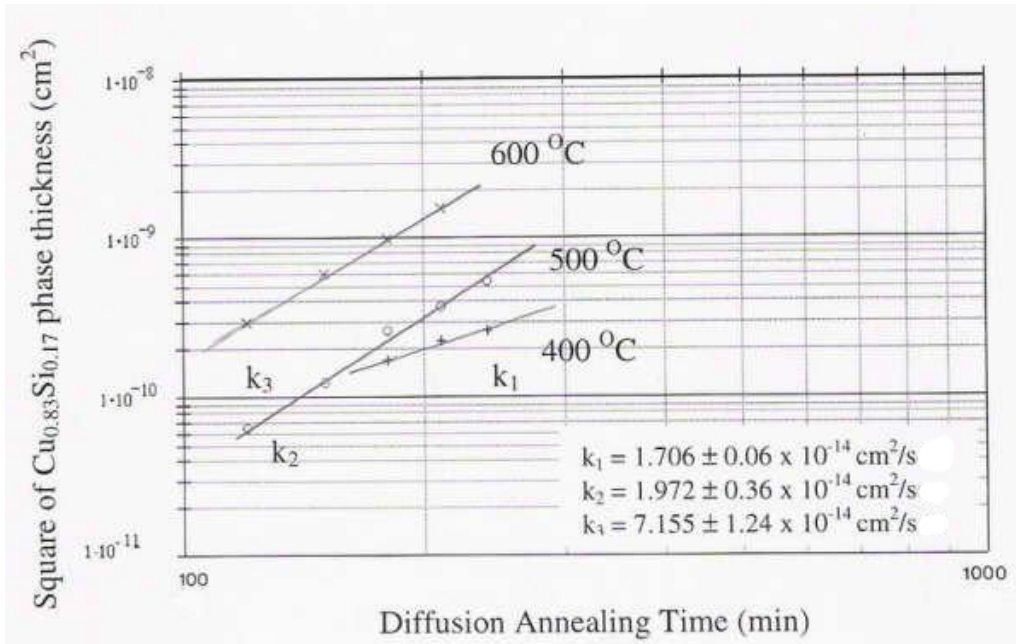


Figure 4. The square of measured phase layer thickness of $\text{Cu}_{0.83}\text{Si}_{0.17}$ versus annealing time (min) on a double logarithmic scale for 400°C, 500°C and 600°C.

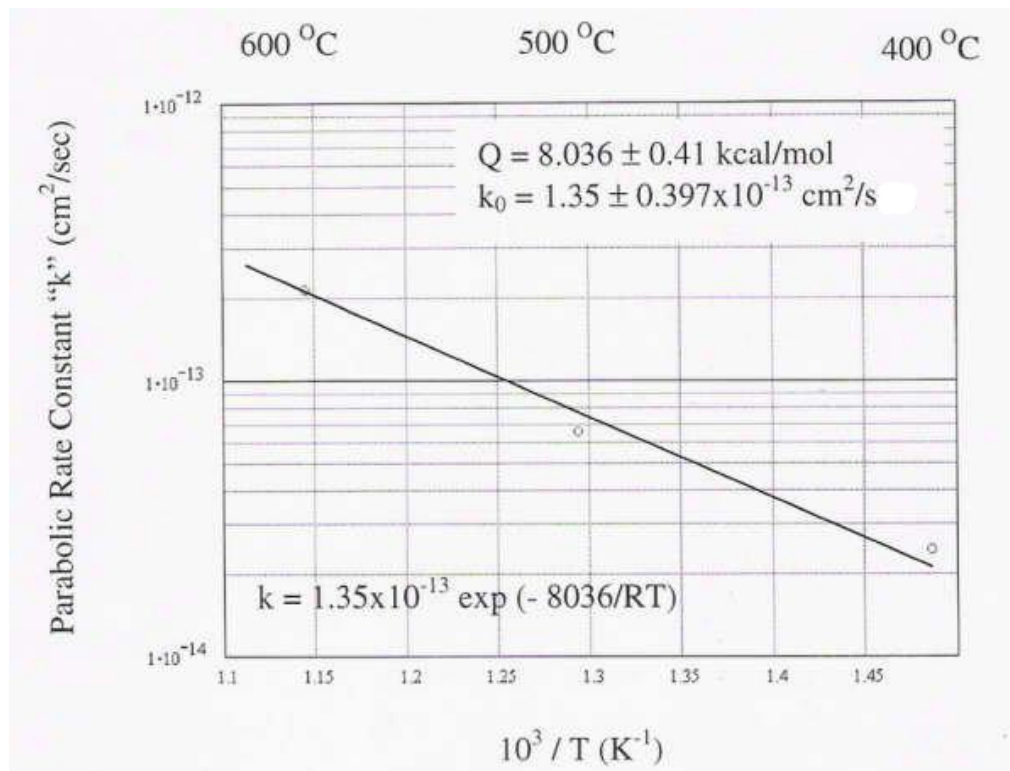


Figure 5. Temperature dependence of the parabolic rate constants for the growth kinetics of the $\text{Cu}_{0.83}\text{Si}_{0.17}$ phase.

Figure 5 shows the plot of $\log(k)$ versus $1/T$ lie on a straight line, so by using Arrhenius relationship;

$$k = k_0 \exp(-Q/RT) \quad (1)$$

where k is the rate constant, k_0 is the preexponential factor, Q is the activation energy, and T is the absolute temperature, Q is 8.036 kcal/mol and the preexponential factor, k_0 , is 1.35×10^{-13} sq cm per sec. As a result; the

below equation which is related to the growth kinetic of $\text{Cu}_{0.83}\text{Si}_{0.17}$ phase can be written as;

$$k = 1.35 \times 10^{-13} \exp(-8036/RT) \text{ cm}^2/\text{s}.$$

3.2. Cu-(5at%)Nb/SiO₂ System

In order to understand impurity effect, (5at%) Nb was added to copper and silicon substrates were deposited by

Cu-(5at%)Nb films having 0.33 μ m thickness, and they were annealed at different temperatures and time intervals. Intermetallic phases formed as Cu_{0.83}Si_{0.17}, Cu₄Si, Nb₅Cu₅Si₄, (Cu, Si) η sequentially at the film-substrate interface were identified from X-Ray diffractograms, SEM micrograph and EDS spectra of Cu-(5at%) Nb films grown on silicon substrates. Those intermetallic phases are listed in Table 3.

X-Ray diffractograms of Cu-(5 at%)Nb films grown on silicon substrate, as-deposited and annealed for 2 h, 2.5 h, 3 h, 3.5 h and 4 h at 500^oC are illustrated in Figure 6. The thickness measurements of Cu_{0.83}Si_{0.17} phase were identified by using SEM micrographs. Thicknesses of the Cu_{0.83}Si_{0.17} layers increase with increasing time and

temperatures as shown in Table 4. The square of measured layer thickness of Cu_{0.83}Si_{0.17} versus diffusion annealing time was plotted on a double logarithmic scale for different temperatures, Figure 7. Experimental points were found to lie on a straight line which implies that reactive diffusion obeys parabolic kinetics and can be expressed by $h^2=k.t$. Parabolic rate constants were determined by the standard method of least squares analysis together with probable errors as in the following;

$$k_1=3.674 \pm 0.036 \times 10^{-14} \text{ cm}^2/\text{s for } 400^{\circ}\text{C}$$

$$k_2=4.363 \pm 0.107 \times 10^{-14} \text{ cm}^2/\text{s for } 500^{\circ}\text{C}$$

$$k_3=4.947 \pm 1.109 \times 10^{-14} \text{ cm}^2/\text{s for } 600^{\circ}\text{C}.$$

Table 3. Phases formed during annealing of Cu-Nb(5 at.%) films on SiO₂ substrates for different temperatures and times (constant thickness of 0.330 μ m).

No	Heat Treatment	Phases Observed
1	As deposited	Cu, Nb, SiO ₂
2	400 ^o C, t=2 h	Cu _{0.83} Si _{0.17} , Cu ₄ Si, SiO ₂
3	400 ^o C, t=2.5 h	Cu, Nb, Cu _{0.83} Si _{0.17} , Cu ₄ Si, SiO ₂
4	400 ^o C, t=3 h	Cu, Nb, Cu _{0.83} Si _{0.17} , Cu ₄ Si, SiO ₂
5	400 ^o C, t=3.5 h	Cu, Nb, Cu _{0.83} Si _{0.17} , Cu ₄ Si, Nb ₅ Cu ₅ Si ₄ , SiO ₂
6	400 ^o C, t=4 h	Cu, Nb, Cu _{0.83} Si _{0.17} , Cu ₅ Si, Nb ₅ Cu ₅ Si ₄ , SiO ₂
7	500 ^o C, t=2 h	Cu, Nb, Cu _{0.83} Si _{0.17} , Cu ₄ Si, Nb ₅ Cu ₅ Si ₄ , SiO ₂
8	500 ^o C, t=2.5 h	Cu, Nb, Cu _{0.83} Si _{0.17} , Cu ₄ Si, Nb ₅ Cu ₅ Si ₄ , (Cu, Si) η , SiO ₂
9	500 ^o C, t=3 h	Cu, Nb, Cu _{0.83} Si _{0.17} , Cu ₄ Si, Nb ₅ Cu ₅ Si ₄ , SiO ₂
10	500 ^o C, t=3.5 h	Cu, Nb, Cu _{0.83} Si _{0.17} , Cu ₄ Si, Nb ₅ Cu ₅ Si ₄ , (Cu, Si) η , SiO ₂
11	500 ^o C, t=4 h	Cu, Nb, Cu _{0.83} Si _{0.17} , SiO ₂
12	600 ^o C, t=2 h	Cu, Nb, Cu _{0.83} Si _{0.17} , SiO ₂
13	600 ^o C, t=2.5 h	Cu, Nb, Cu _{0.83} Si _{0.17} , SiO ₂
14	600 ^o C, t=3 h	Cu, Nb, Cu _{0.83} Si _{0.17} , SiO ₂
15	600 ^o C, t=3.5 h	Cu, Nb, Cu _{0.83} Si _{0.17} , Nb ₅ Cu ₅ Si ₄ , SiO ₂
16	600 ^o C, t=4 h	Cu, Nb, Cu _{0.83} Si _{0.17} , Cu ₄ Si, Nb ₅ Cu ₅ Si ₄ , (Cu, Si) η , Cu ₅ Si, SiO ₂

Table 4. Thickness variation in μ m with time and temperature of Cu_{0.83}Si_{0.17} layer in Cu-(5at%)Nb / Si system.

Temp.	Time				
	2 h	2.5 h	3 h	3.5 h	4 h
400 ^o C	0.16	0.18	0.20	0.22	0.23
500 ^o C	0.18	0.19	0.21	0.24	0.26
600 ^o C	0.19	0.20	0.23	0.26	0.27

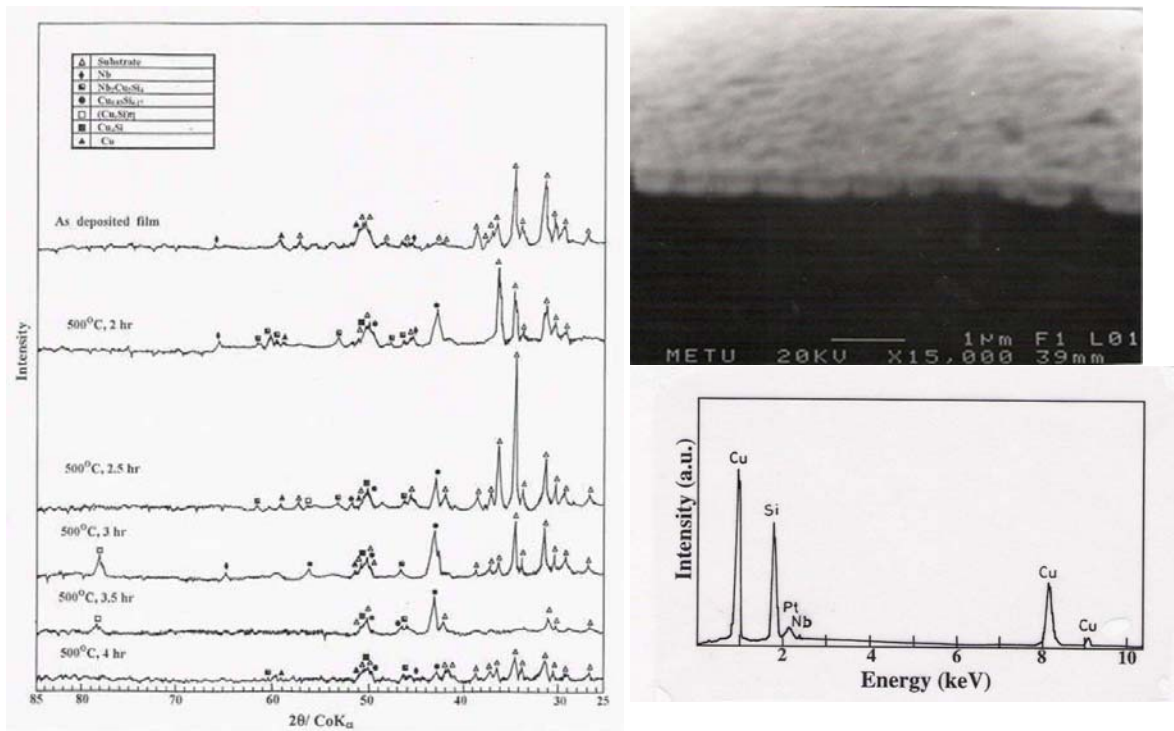


Figure 6. a-) X-Ray diffractograms of Cu-(5 at%)Nb films grown on silicon substrate, as deposited and annealed for 2 h, 2.5 h, 3 h, 3.5 h and 4 h at 500°C., b-) SEM micrograph of 0.33 μm thick Cu film grown on silicon substrate as-deposited; c-) EDS spectrum of the same film.

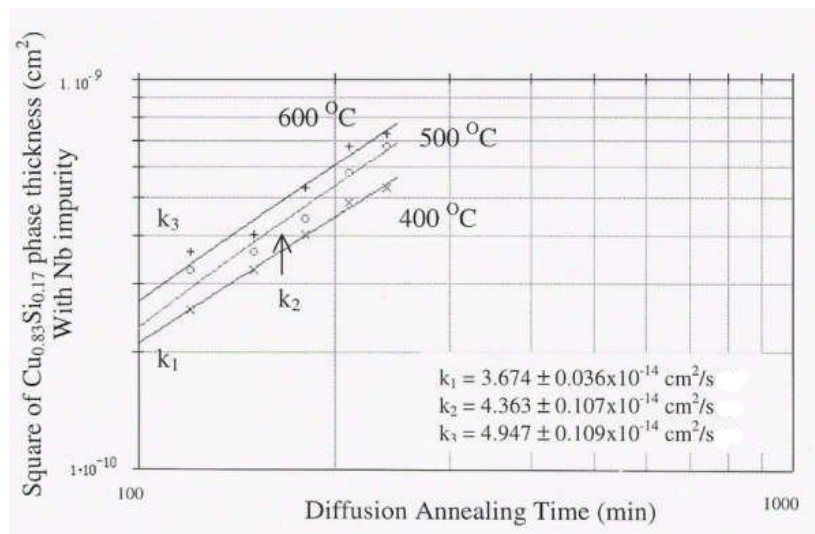


Figure 7. The square $\text{Cu}_{0.83}\text{Si}_{0.17}$ phase thickness (cm^2) with Nb impurity versus diffusion annealing time (min) on a double logarithmic scale for 400°C, 500°C and 600°C.

Figure 8 shows the plot of $\log(k)$ versus $1/T$ lie on a straight line which obeys Arrhenius relationship.

By using Arrhenius relationship;

$$k = k_0 \exp(-Q/RT) \tag{2}$$

where k is the rate constant, k_0 is the preexponential factor, Q is the activation energy, and T is the absolute temperature, the below equation which is related to the

growth kinetic of $\text{Cu}_{0.83}\text{Si}_{0.17}$ phase formed at Cu-(5at%)Nb/Si interface, can be written as:

$$k = 1.35 \times 10^{-13} \exp(-1738/RT) \tag{3}$$

After addition of (5at%)Nb to the Cu-Si system; parabolic rate constants increased and activation energy values decreased from the value 8.036 ± 0.41 kcal/mol to the value 1.738 ± 0.056 kcal/mol.

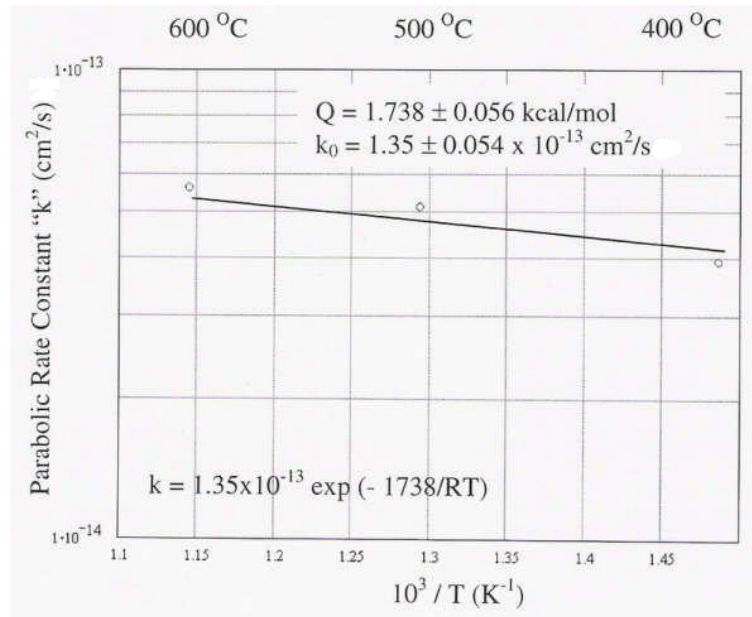


Figure 8. Temperature dependence of the parabolic rate constants for the growth kinetics of $\text{Cu}_{0.83}\text{Si}_{0.17}$ phase with Nb impurity.

4. CONCLUSIONS

The main conclusions deduced from this work on the intermetallic compound formation at Cu-Si and Cu-(5at%)Nb/Si interfaces may be summarized as follows:

1- XRD, SEM and EDS analysis showed sequential formation of several intermetallic phases at the interfaces. On the contrary, intermetallic phases are simultaneously formed in bulk materials.

2- Intermetallics; $\text{Cu}_{0.83}\text{Si}_{0.17}$, Cu_4Si , $(\text{Cu}, \text{Si})\eta$ and $(\text{Cu}, \text{Si})(\text{Si at}\%21.2)$, were determined in Cu/Si system. In Cu-(5at%)Nb/Si system, intermetallics; $\text{Cu}_{0.83}\text{Si}_{0.17}$, Cu_4Si , $\text{Nb}_5\text{Cu}_5\text{Si}_4$, $(\text{Cu}, \text{Si})\eta$ and $(\text{Cu}, \text{Si})(\text{Si at}\%21.2)$, were observed.

3- Experimental results implied that the reactive diffusion obeys parabolic growth kinetics and can be expressed by $h^2=kt$; where h is the thickness of $\text{Cu}_{0.83}\text{Si}_{0.17}$ phase, k is the parabolic rate constant, and t is the diffusion annealing time.

4- Parabolic rate constants were determined by the standard method of least squares analysis. From the calculations, Arrhenius type equations can be given as:

For the growth kinetics of $\text{Cu}_{0.83}\text{Si}_{0.17}$ layer in Cu/Si system;

$$k=1.35 \times 10^{-13} \exp(-8036/RT) \text{ cm}^2/\text{s}$$

and for the growth kinetics of $\text{Cu}_{0.83}\text{Si}_{0.17}$ layer in Cu-(5at%)Nb/Si system;

$$k=1.35 \times 10^{-13} \exp(-1740/RT) \text{ cm}^2/\text{s}$$

5- Parabolic rate constants increase with Nb impurity content and activation energies decrease.

ACKNOWLEDGEMENTS

This work had been realised in Metallurgical and Materials Engineering Department of Middle East

Technical University, and I'd like to thank laboratory personnel of the department who contribute to this work.

REFERENCES

- [1] Wang, Y., Gao, G., "Synthesis and enhanced intercalation properties of nanostructured vanadium oxides", *Chemistry of Materials*, 18(12):2787-2804 (2006).
- [2] Selvan, R.K., Kalaiselvi, N., Augustin, C.O., Doh, C.H., "SnO₂ pinning: An approach to enhance the electrochemical properties of nanocrystalline CuFe₃O₄ for lithium-ion batteries", *Electrochemical and Solid State Letters*, 9(8):A390-A394 (2006).
- [3] Kim, S., Cianfrone, J.A., Sadik, P., Kim, K.W., Ivil, M., Norton, D.P., "Room temperature deposited oxide p-n junction using p-type zinc-cobalt-oxide", *Journal of Applied Physics*, 107(10): 103538 (2010).
- [4] Erdogan, I.Y., Gullu, O., "Silicon MIS diodes with Cr₂O₃ nanofilm: Optical, morphological/structural and electronic transport properties", *Applied Surface Science*, 256(13): 4185-4191(2010).
- [5] Tavares, C.J., Marques, S.M., Rebouta, L., Lanceros-Mendez, S., Sencadas, V., Costa, C.M., Alves, E., Fernandes, A.J., "PVD-Grown photocatalytic TiO₂ thin films on PVDF substrates for sensors and actuators applications", *Thin Solid Films*, 517: 1161-1166(2008).
- [6] Liu, H.K., Wang, G.X., Guo, Z.P., Wang, J.Z., Konstantinov, K., "Nanomaterials for lithium-ion rechargeable batteries", *Journal of Nanoscience and Nanotechnology*, 6: 1-15(2006).
- [7] Freiman, G., Barbour, P., Perrière, J., Giannakopoulos, K., "Layer by layer deposition of

- zirconium oxide onto silicon”, *Thin Solid Films*, 517: 2670-2674 (2009).
- [8] Murarka, S.P., Blech, I.A., Levistein, H.J., “Thin-film interaction in aluminum and platinum”, *J. Appl. Phys.*, 47: 5175-5181 (1976).
- [9] Nakamura, K., Nicolet, M.A., Mayer, J., Blattner, R.J., Evans, C.A., “Interaction of Al layers with polycrystalline Si”, *J. Appl. Phys.*, 46: 4678-4684 (1975).
- [10] Nakamura, K., Olowolafe, J.O., Lau, S.S., Nicolet, M.A., Mayer, J.W., “Interaction of metal layers with polycrystalline Si”, *J. Appl. Phys.*, 47:1278-1283 (1976).
- [11] Locker, L.D., Capio, C.D., “Reaction kinetics of tungsten thin films on silicon (100) surfaces”, *J. Appl. Phys.*, 44: 4366-4369(1973).
- [12] Tan, Z.Q., Heald, S.M., “Interfacial reactions between nickel–chromium alloys and aluminum”, *J. Appl. Phys.*, 71: 3766-3772 (1992).
- [13] Lee, C.C., Machlin, E.S., Rathore, H.J., “Roles of Ti-intermetallic compound layers on the electromigration resistance of Al-Cu interconnecting stripes”, *J. Appl. Phys.*, 71: 5877-5887 (1992).
- [14] Padiyath, R., Seth, J., Babu, S.V., Matienzo, L.J., “Deposition of copper films on silicon substrates: Film purity and silicide formation”, *J. Appl. Phys.*, 73: 2326-2332(1992).
- [15] Liu, C.S., Chen, L.J., “Interfacial reactions of ultrahigh-vacuum-deposited Cu thin films on atomically cleaned (111)Si. I. Phase formation and interface structure”, *J. Appl. Phys.*, 74: 5501-5506 (1993).
- [16] Agilan, S., Mangalaraj, D., Narayandass, S.A.K., Mohen Rao, G., Velumani, S., “Structure and temperature dependence of conduction mechanisms in hot wall deposited CuInSe₂ thin films and effect of back contact layer in CuInSe₂ based solar cells.”, *Vacuum*, 84(10): 1220-1225 (2010).
- [17] Quang, P.H., Yu, S.C., “Effect of substrate temperature and annealing process on the transport property of Al_{0.87}Mn_{0.13}N thin films.”, *Journal of the Korean Physical Society*, 52(5):1669-1672 (2008).
- [18] Aksu, M.A., Yakıncı, M.E., Güldeste, A., “Co-addition into MgB₂: The structural and electronic properties of (MgB₂)_{2-x}Co_x”, *Journal of Alloys and Compounds*, 424(1-2):33-40 (2006).
- [19] Fadel, M., Sedeek, K., Hegab, N.A., “Effect of Sn content on the electrical and optical properties of Ge_{1-x}Sn_xSe₃ glasses”, *Vacuum*, 57(3):307-317 (2000).
- [20] Guler (Yaroglu), H., “Formation of Intermetallic Phases at the Metal – Silicon Interfaces”, Ph.D. Thesis, *Middle East Technical University, Graduate School of Natural Applied Sciences*, (2001).
- [21] Ozenbas, M., Guler, H., “Formation of Al-Si Intermetallic Phases”, *Chemical Engineering Communications*, 190(5): 911 – 924(2003).